

ISSN: 0256-307X

中国物理快报

Chinese Physics Letters

Volume 34 Number 9 September 2017

A Series Journal of the Chinese Physical Society
Distributed by IOP Publishing

Online: <http://iopscience.iop.org/0256-307X>
<http://cpl.iphy.ac.cn>

CHINESE PHYSICAL SOCIETY
IOP Publishing

JUST FOR AUTHORS
— CHINESE PHYSICS LETTERS

Nonresonant and Resonant Nonlinear Absorption of CdSe-Based Nanoplatelets *

Li-Bo Fang(方立波), Wei Pan(潘葳)**, Si-Hua Zhong(钟思华), Wen-Zhong Shen(沈文忠)**

Laboratory of Condensed Matter Spectroscopy and Opto-Electronic Physics, and Key Laboratory of Artificial Structures and Quantum Control (Ministry of Education), School of Physics and Astronomy, Shanghai Jiao Tong University, Shanghai 200240

(Received 27 April 2017)

We present a comprehensive understanding of the nonlinear absorption characteristics of CdSe-based nanoplatelets (NPLs) synthesized by the solution-phase method and the colloidal atomic layer deposition approach through Z-scan techniques at 532 nm with picosecond pulses. The CdSe NPLs exhibit strong two-photon induced free carrier absorption (effective three-photon absorption) upon the nonresonant excitation, resulting in a remarkable optical limiting behavior with the limiting threshold of approximately 75 GW/cm^2 . A nonlinear optical switching from saturable absorption (SA) to reverse saturable absorption (RSA) with increasing the laser intensity is observed when coating CdSe NPLs with a monolayer of CdS shell to realize the resonant absorption. The SA behavior originates from the ground state bleaching and the RSA behavior is attributed to the free carrier absorption. These findings explicitly demonstrate the potential applications of CdSe-based NPLs in nonlinear optoelectronics such as optical limiting devices, optical pulse compressors and optical switching devices.

PACS: 81.05.Dz, 81.07.-b, 42.65.-k, 42.70.Nq, 78.67.-n

DOI: 10.1088/0256-307X/34/9/098101

Colloidal semiconductor nanocrystals possess large optical nonlinearity due to the quantum confinement effect, and their nonlinear optical parameters can be conveniently tuned by their sizes, shapes and compositions.^[1–3] Therefore, colloidal semiconductor nanocrystals are believed to be the promising materials for the applications in nonlinear gain media,^[4,5] optical limiting,^[6,7] all optical switching,^[8,9] and biolabeling.^[10] Up to now, extensive work has been performed on the nonlinear optical properties of semiconductor nanocrystals, especially the different-shaped II–VI semiconductor nanocrystals, such as CdSe quantum dots (QDs),^[11] CdSe/ZnS core/shell QDs,^[11] CdS nanorods (NRs),^[12] and CdSe/CdS core/shell NRs.^[13]

CdSe-based nanoplatelets (NPLs), as one of the new members in II–VI semiconductor nanocrystals, possess large lateral size and small thickness easily controlled at atomic precision,^[14] and have attracted a great deal of attention for their superior optical and electronic properties. Theoretical investigation has indicated that the increase of lateral size is advantageous to enhance the nonlinear optical effect.^[15] A recent experiment has demonstrated that CdSe NPLs show 10 times more efficient two-photon absorption (2PA) than their NRs and QDs counterparts by open aperture (OA) Z-scan at femtosecond 800 nm laser,^[2] arising from the high two-dimensional density of states and the ultra-strong anisotropic confinement. However, the nonlinear optical absorption of CdSe NPLs strongly depends on the electronic transition properties of the material and the excitation parameters (energy, pulse duration and irradiance of the incident laser beam).^[16] It is highly necessary to comprehensively understand the nonlinear optical characteristics

of CdSe-based NPLs working at nonresonance as well as at resonance so that we can better apply them to nonlinear optoelectronics.

In this work, we explore the nonlinear absorption behaviors of the CdSe-based NPLs using the Z-scan technique with an incident laser beam of 532 nm in the picosecond (ps) region. We find that the nonlinear absorption of CdSe NPLs is dominated by the two-photon induced free carrier absorption (FCA) in nonresonant regime and can incur remarkable optical limiting behavior. Nevertheless, by coating CdSe NPLs with CdS shell (namely CdSe/CdS core/shell NPLs) for the resonant excitation, the nonlinear absorption is able to be tuned from saturable absorption (SA) to reverse saturable absorption (RSA) by the input laser intensity, which provides the potential applications in optical pulse compressors and optical switching devices.

The synthesis of CdSe NPLs was performed by the solution-phase method with slight modification.^[14] In a typical synthesis, 480 mg of cadmium acetate dihydrate $[\text{Cd}(\text{Ac})_2 \cdot 2\text{H}_2\text{O}]$, 1.18 g of oleic acid, and 90 mL of 1-octadecene (ODE) were mixed in a 250-mL three-neck flask and degassed under a vacuum at 110°C for 90 min. After that, 72 mg of selenium powder dispersed in 2 mL of ODE was injected in an argon atmosphere. When temperature reached 180°C , 240 mg of $\text{Cd}(\text{Ac})_2 \cdot 2\text{H}_2\text{O}$ was introduced and then the mixture was heated at 240°C for 10 min. After cooling down, the NPLs were washed with ethanol and redispersed in hexane. To realize the resonant excitation, these CdSe NPLs were then coated with a monolayer of CdS shell on both sides to form CdSe/CdS core/shell NPLs by a colloidal atomic layer deposition approach to grow CdS shell with high quality.^[17] This step is useful in

*Supported by the National Natural Science Foundation of China under Grant Nos 61234005 and 11304197.

**Corresponding author. Email: sjtushelwill@sjtu.edu.cn; wzshen@sjtu.edu.cn

© 2017 Chinese Physical Society and IOP Publishing Ltd

adjusting the excitonic absorption energy by changing the confinement barriers, and is also helpful to increase the photo- and chemical-stability by protecting the NPLs.^[17] To obtain it, 200 μL of as-prepared CdSe NPLs (~ 20 mg/mL) were mixed with 2 mL of N-methylformamide (NMF), 4 μL of ammonium sulfide aqueous solution (20%), and 2 mL of hexane to coat S^{2-} ions on the surface of CdSe NPLs. After phase transfer, the polar phase was washed three times with hexane, precipitated with acetonitrile, and redispersed in NMF. Then 30 μL of 0.1 mol/L $\text{Cd}(\text{Ac})_2 \cdot 2\text{H}_2\text{O}$ solution in NMF was added and stirred for 1 min to finish the growth of one monolayer of CdS. Finally, 50 μL of oleylamine and 2 mL of hexane were added into the well-washed CdSe/CdS core/shell NPLs in NMF to finish the phase transfer from NMF to hexane. The extra oleylamine was removed by washing with ethanol.

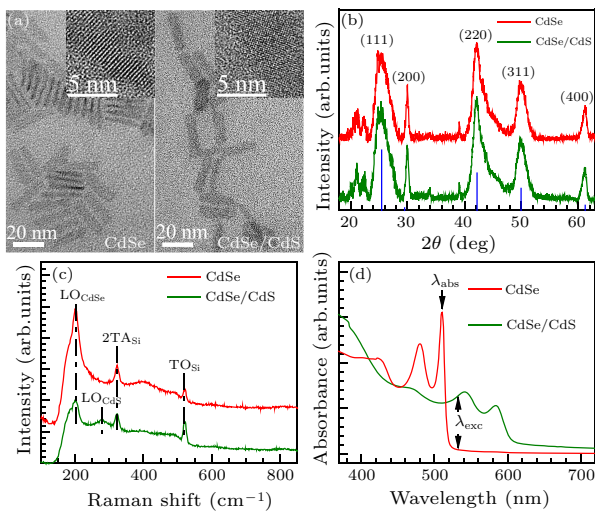


Fig. 1. Structure and optical properties of CdSe and CdSe/CdS core/shell NPLs. (a) TEM images, (b) XRD patterns, (c) Raman spectra, and (d) linear absorption spectra. Inset of (a) is the HRTEM images. The blue line in (b) represents the standard XRD patterns of zinc blende bulk CdSe.

The morphology and microstructure of the NPLs were characterized by high resolution transmission electron microscopy (HRTEM, JEOL JEM-2100 F). The crystal structure and chemical composition were measured by x-ray diffraction (XRD, Bruker D8 Advance) and room-temperature Raman spectroscopy (Jobin Yvon LabRAM HR 800UV micro-Raman spectrometer) with a 325 nm He-Cd laser. The absorption spectra were collected at room temperature on a Perkin Elmer Lambda 35 spectrometer. The concentration of the NPL solution was determined using inductively coupled plasma optical emission spectroscopy (ICP-OES, Thermo Scientific ICAP 6300) after dissolving NPLs in nitric-acid.^[5,18,19] The nonlinear optical absorption was investigated by the traditional OA *Z*-scan measurements.^[20] The light source was a Q-switched neodymium doped yttrium aluminum garnet (Nd: YAG) laser, operating at a wavelength of 532 nm with the pulse width of 15 ps, the

repetition rate of 10 Hz. The transverse distribution of the laser beam has a nearly Gaussian profile and the temporal profile is also nearly Gaussian shape. The pulses were focused by a convex lens with a focal length of 400 mm, producing a beam waist at the focus $\omega_0 \sim 20$ μm . The CdSe-based NPLs dispersed in hexane were filled in 1 mm quartz cuvettes and then mounted on a computer-controlled translation stage.

Figure 1(a) displays the transmission electron microscopy (TEM) images of the CdSe and CdSe/CdS core/shell NPLs, together with their HRTEM images in the inset. The HRTEM images exhibit the crystallinity of CdSe and CdSe/CdS core/shell NPLs. Statistical analysis of TEM images gives the average lateral sizes of CdSe (7 nm \times 22 nm) and CdSe/CdS core/shell (7 nm \times 23 nm) NPLs. Obviously, the lateral sizes of NPLs almost keep unchanged after the coating of CdS shell. The XRD patterns in Fig. 1(b) show that the CdSe NPLs possess typical diffraction peaks of (111), (200), (220), (311) and (400) planes of zinc blende CdSe. Interestingly, the XRD spectrum of CdSe/CdS core/shell NPLs is identical to that of CdSe NPLs. It suggests that the growth of CdS shell on CdSe core is epitaxial and coherent. Due to the coherency strain, the coated CdS monolayer adopts the lattice parameters of CdSe core to form a dislocation-free interface.^[21] The existence of CdS monolayer is directly observed from the Raman spectra in Fig. 1(c). As shown in this figure, both the spectra of CdSe and CdSe/CdS core/shell NPLs display the typical longitudinal optical (LO) phonon mode of CdSe at 202.1 cm^{-1} .^[22] Moreover, the Raman spectrum of CdSe/CdS core/shell NPLs also shows an additional peak at 277.2 cm^{-1} , which is assigned to the monolayer of CdS formed on the surface of CdSe NPLs.^[22] This value of 277.2 cm^{-1} is far away from the LO phonon energy (297 cm^{-1}) of bulk CdS, further indicating the existence of the coherency strain. Figure 1(d) gives the absorption spectra of CdSe and CdSe/CdS NPLs. Both of them exhibit sharp band-edge absorption and two well-resolved excitonic transitions, i.e., electron/heavy-hole (low energy) and electron/light-hole transition (high energy). The sharp band-edge absorption, instead of band-tail absorption, together with the excitonic transition, suggests the good crystallinity of CdSe and CdSe/CdS NPLs. Due to the addition of a single CdS layer to both sides of CdSe NPLs, electron wave functions in CdSe are delocalized into the CdS shell, thus the electron confinement energy in CdSe/CdS NPLs is weaker than that in CdSe NPLs.^[17] Correspondingly, the excitonic transition redshifts, e.g., λ_{abs} shifts from 510 to 584 nm.

Figure 2(a) shows the *Z*-scan transmission spectra (open circles) of the CdSe NPLs in hexane with a concentration of 4.0×10^{-7} mol/L. The excitation intensities of ps 532 nm laser (nonresonant excitation) varied from 19 to 109 GW/cm^2 . Similar measurements were performed on the pure solvent (hexane) and no clear

Z-scan curves were recorded, validating that the measured nonlinear absorption originates from the CdSe NPLs only. As shown in the figure, all the OA Z-scan data exhibit a decrease of transmittance with respect to the focus, indicating the occurrence of multiphoton absorption.^[23] We attempt to fit the experimental data according to the following equations under the assumption of pure 2PA and pure three-photon absorption (3PA),^[24] respectively,

$$T_{\text{OA}(2\text{PA})}(z) = \frac{1}{\pi^{1/2}q_0} \int_{-\infty}^{\infty} \ln[1 + q_0 \exp(-x^2)] dx, \quad (1)$$

$$T_{\text{OA}(3\text{PA})}(z) = \frac{1}{\pi^{1/2}p_0} \int_{-\infty}^{\infty} \ln\{[1 + p_0^2 \exp(-2x^2)]^{1/2} + p_0 \exp(-x^2)\} dx, \quad (2)$$

where $T_{\text{OA}(n\text{PA})}$ is the normalized OA transmittance with n being the number of photons involved in the nonlinear absorption process, $q_0 = \beta I_0 L_{\text{eff}}$ with β being the 2PA coefficient, $I_0 = I_{00}/(1 + z^2/z_0^2)$ the excitation intensity at position z (I_{00} is the laser peak intensity at the focal point, and $z_0 = \pi\omega_0^2/\lambda$ is the Rayleigh length), and the 2PA effective sample length $L_{\text{eff}} = [1 - \exp(-\alpha_0 L)]/\alpha_0$ with L being the sample thickness; as well as $p_0 = (2\gamma I_0^2 L'_{\text{eff}})^{1/2}$ with γ being the 3PA coefficient and the 3PA effective sample

length $L'_{\text{eff}} = [1 - \exp(-2\alpha_0 L)]/2\alpha_0$.

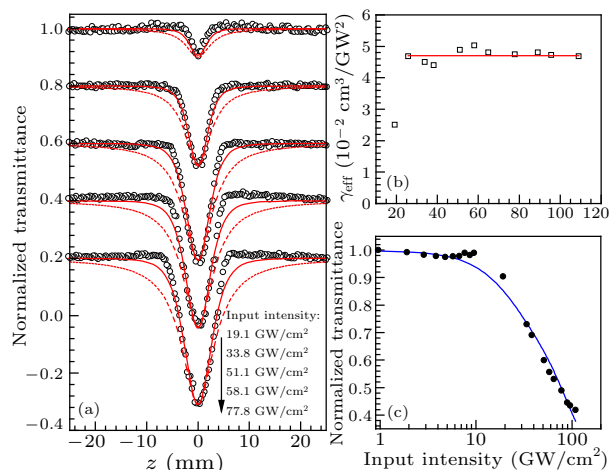


Fig. 2. (a) Stacked OA Z-scan data (open circles) of the CdSe NPLs in hexane at different input intensities. The dashed and solid curves are the fits using the 2PA and 3PA theories, respectively. For clarification, the curves are shifted along the vertical direction, and each curve is separated by 0.2. (b) Intensity dependence of the effective 3PA coefficients γ_{eff} for the CdSe NPLs. The solid line is a guide for the eyes. (c) Nonlinear transmittance of the CdSe NPLs as a function of the input intensity. The circles are the experimental data and the line is the theoretical fitting using the three-level two-step 3PA model.

Table 1. Relevant parameters (γ_{eff} , I_s , β_{eff}) obtained by the best theoretical fits of experimental data for CdSe and CdSe/CdS core/shell NPLs at different excitation peak intensities (I_{00}).

CdSe NPLs		CdSe/CdS core/shell NPLs		
I_{00} (GW/cm ²)	γ_{eff} (cm ³ /GW ²)	I_{00} (GW/cm ²)	I_s (GW/cm ²)	β_{eff} (cm/GW)
19.1	2.5×10^{-2}	3.9	0.09	1.4×10^{-8}
33.8	4.5×10^{-2}	7.8	0.11	0.72
51.1	4.8×10^{-2}	17.3	0.45	0.83
58.1	5.0×10^{-2}	27.0	1.25	0.86
77.8	4.7×10^{-2}			

The dashed curves in Fig. 2(a) are the theoretical fits using the 2PA theory (Eq. (1)) and it is obvious that they deviate from the experimental observation. Nevertheless, the solid curves obtained using the 3PA theory (Eq. (2)) agree well with the experimental data. Relevant parameters used in the fits are listed in Table 1. Achtstein *et al.*^[12] have also observed the similar results in CdS QDs and modelled their data using an instantaneous 3PA coefficient. In our case, as the excitation wavelength (λ_{exc}) used for the measurements fulfills the requirement ($\lambda_{\text{abs}} < \lambda_{\text{exc}} < 2\lambda_{\text{abs}}$) for 2PA studies at 532 nm, the absorption mechanism here should be two-photon resonant 3PA,^[25] i.e., effective 3PA. Figure 3(a) represents the schematic energy level diagram for the CdSe NPLs to explain the nonlinear processes. In the nonresonant regime, excited electrons transit from the valence band to the conduction band through an instantaneous 2PA process. Subsequently, the free charge carriers can be further excited to the higher conduction band states through a third photon, which is called FCA or excited state absorption (ESA). The whole process described above is called the effective 3PA since the two-photon induced

FCA or ESA is a three-photon process. Sutherland *et al.*^[26] have also successfully explained the two-photon induced ESA in organic chromophores with an effective 3PA model. The effective 3PA coefficients γ_{eff} were evaluated from the best fits using the 3PA theory (Eq. (2)) as shown in Fig. 2(b). It is obvious that the measured γ_{eff} values almost keep as a constant of 4.7×10^{-2} cm³/GW² with the input intensities upon 25 GW/cm², which demonstrates the validity of the effective 3PA process.

Since the effective 3PA is actually a two-photon induced FCA, we try to separate the contributions of 2PA and FCA. Here 2PA is a third-order nonlinear absorption process, while FCA can be considered as a fifth-order nonlinear absorption in theoretical treatment. Therefore, a three-level two-step 3PA model^[27] has been proposed to separate them when considering the whole absorption coefficient α as $\alpha_0 + \beta I + \gamma I^2$. For this purpose, we show in Fig. 2(c) the normalized transmission $T(0)$ at the focus as a function of the input intensity I_{00} . The solid blue line is the fitting result using the three-level two-step 3PA model.^[27] The least-square fitting yields a 2PA

coefficient β of $0.0584 \text{ cm}^2/\text{GW}$ and an FCA-related 3PA coefficient γ of $0.0304 \text{ cm}^3/\text{GW}^2$. The 2PA cross section $\sigma_{2\text{PA}}$ per CdSe NPL is calculated to be $9.04 \times 10^{-44} \text{ cm}^4 \cdot \text{s}/\text{photon}$ (or $9.04 \times 10^6 \text{ GM}$) using the relation of $\sigma_{2\text{PA}} = (h\nu/C)\beta$, where $h\nu$ is the photon energy and C the particle concentration. The FCA cross section is estimated to be $\sigma_{\text{F}} = 1.94 \times 10^{-16} \text{ cm}^2$ via the formula of $\gamma = \sigma_{\text{F}}\beta\tau_{\text{F}}/2h\nu$ after taking the free carrier lifetime $\tau_{\text{F}} \sim 2 \text{ ps}$.^[28] Apparently, once the input intensity is larger than $10 \text{ GW}/\text{cm}^2$, the contribution from the FCA is much larger than that from 2PA for $\gamma I \gg \beta$, suggesting the effectiveness of the 3PA model in Fig. 2(a).^[26] Furthermore, Fig. 2(c) also displays an obvious optical limiting behavior of the CdSe NPLs. With an input intensity of less than $10 \text{ GW}/\text{cm}^2$, the energy transmittance is almost a constant. However, in excess of $10 \text{ GW}/\text{cm}^2$, the transmittance decreases when we increase the input intensity, showing a typical limiting property.^[29] The limiting threshold, defined as the input intensity at which the transmittance decreases to half the linear transmittance, is approximately $75 \text{ GW}/\text{cm}^2$.

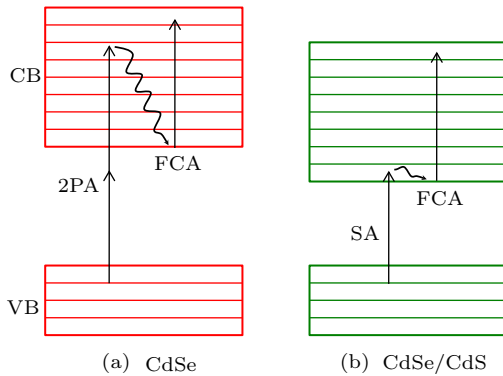


Fig. 3. Schematic diagram of the energy level for (a) CdSe NPLs in the nonresonant regime and (b) CdSe/CdS core/shell NPLs in the resonant region. VB: valence band; CB: conduction band; 2PA: two-photon absorption; FCA: free carrier absorption; SA: saturable absorption.

The nonlinear absorption behavior of NPLs was also studied in the resonant regime by coating CdSe NPLs with CdS shells to lower the required excitation energy. Figure 4 presents the nonlinear absorption curves for the CdSe/CdS core/shell NPLs in hexane with the concentration of $1.4 \times 10^{-7} \text{ mol/L}$ excited at different input intensities. At a relatively low intensity of $3.9 \text{ GW}/\text{cm}^2$ as shown in Fig. 4(a), the normalized transmittance increases monotonically with the sample closing to the focus, suggesting the SA behavior. Figure 4(b) shows the nonlinear absorption curve obtained at a relatively higher intensity of $7.8 \text{ GW}/\text{cm}^2$. With closing to the focus, the transmittance increases at first (SA behavior), then decreases near the focus which shows the RSA behavior. The transition from SA to RSA results in an absorption curve with a symmetrical valley and two humps. With the further increase of the input intensity (Figs. 4(c) and 4(d)), the humps drive down while the depth of the valley increases, indicating a stronger RSA.

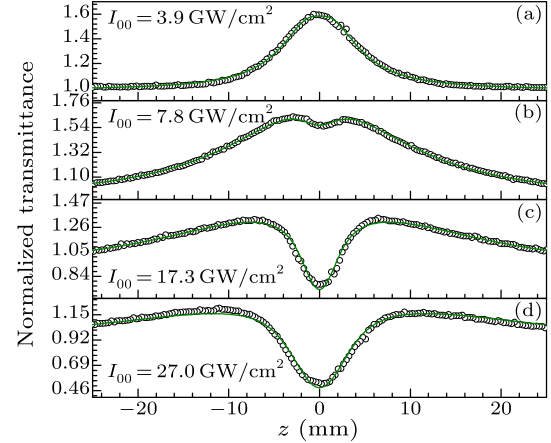


Fig. 4. OA Z-scan experimental data (open circles) and theoretical fits (solid lines) of the CdSe/CdS core/shell NPLs at different excitation peak intensities: (a) $3.9 \text{ GW}/\text{cm}^2$, (b) $7.8 \text{ GW}/\text{cm}^2$, (c) $17.3 \text{ GW}/\text{cm}^2$, and (d) $27.0 \text{ GW}/\text{cm}^2$.

A schematic energy level diagram for the CdSe/CdS core/shell NPLs as shown in Fig. 3(b) is used to explain the above nonlinear absorption processes in the resonant regime. In CdSe NPLs, the electron and hole wave functions are strongly confined along the direction of thickness, exhibiting discrete electron and hole energy levels. In CdSe/CdS core/shell NPLs, the holes are still confined in the CdSe core while the electron could easily move between CdSe and CdS,^[17] since the conduction band offset between CdSe and CdS is small but their valence band offset is large.^[30] Therefore, the hole energy levels in CdSe/CdS NPLs are almost the same to those in CdSe NPLs, but their electron energy levels are lowered down, as shown in Fig. 3. The shift of energy levels in CdSe/CdS NPLs finally leads to a redshift of the first excitonic transition from 510 to 584 nm (Fig. 1(d)). Because the excitation energy is larger than the excitonic absorption peak energy of CdSe/CdS core/shell NPLs, the electron can be directly excited from the ground state to the excited state by absorbing one photon with a wavelength of 532 nm . When the input intensity is low, the absorption in the ground state is saturated and thereby results in a strong SA behavior. However, when the input intensity is sufficiently high, the FCA will play an important role, leading to an effective 2PA and thus the RSA behavior. Note that, the SA behavior of the sample at the position far away from the focal point is due to the declined light intensity. Such type of switching behavior has also been observed in CdSe QDs,^[31] Bi_2S_3 NRs,^[32] and gold nanocubes.^[33]

To obtain an insight into the transition of nonlinear absorption behavior of the CdSe/CdS core/shell NPLs at different input intensities, we present the total absorption coefficient $\alpha(I)$,^[34]

$$\alpha(I) = \alpha_0 \frac{1}{1 + I/I_s} + \beta_{\text{eff}} I, \quad (3)$$

where the first term describes the SA, and the second

term describes the RSA resulting from the effective 2PA. The linear absorption coefficient α_0 is 8.9 cm^{-1} for the CdSe/CdS core/shell NPLs at 532 nm. Here I is the laser intensity as functions of r , t and z , with r being the radial distance from the optical axis and t the time, I_s is the saturation intensity, β_{eff} is the effective 2PA coefficient, and I in the sample obeys the following differential equation,^[20]

$$\frac{dI}{dz'} = -\alpha(I)I, \quad (4)$$

where z' is the propagation distance inside the sample. The normalized transmittance at the sample position z for OA Z -scan is expressed as^[20]

$$T(z) = \frac{\int_{-\infty}^{+\infty} dt \int_0^{+\infty} I_{\text{out}} r dr}{\exp(-\alpha_0 L) \int_{-\infty}^{+\infty} dt \int_0^{+\infty} I_{\text{in}} r dr}, \quad (5)$$

where I_{out} is the laser intensity at the output plane, which can be represented as an infinite series from solving Eqs. (3) and (4) using the Adomian decomposition method,^[35] $I_{\text{in}} = I_{00} \frac{\omega_z^2}{\omega_0^2} \exp(-\frac{2r^2}{\omega_z^2}) \exp(-\frac{t^2}{\tau^2})$ is the laser intensity at the entrance plane of the sample with $\omega_z^2 = \omega_0^2(1 + z^2/z_0^2)$ being the beam radius and τ the input pulse width.

The solid curves in Fig. 4 are the best theoretical fits of the experimental data through Eq. (5), and the corresponding nonlinear coefficients I_s and β_{eff} are listed in Table 1. Similar to those observed in CdSe-based QDs and nc-Si: H,^[31,36] both I_s and β_{eff} increase with I_{00} . The I_{00} -dependent I_s and β_{eff} values reflect the competition between the ground state absorption and the FCA. At a low I_{00} , the ground state absorption dominates and leads to the SA behavior. With the increase of I_{00} , the FCA process gradually plays an important role and more electrons can be excited to the conduction band from the valence band, leading to increasing I_s and β_{eff} . At a sufficiently high I_{00} , the FCA process dominates and incurs the RSA behavior. For example, at $I_{00} = 3.9\text{ GW/cm}^2$, I_s is calculated to be 0.09 GW/cm^2 and β_{eff} is almost 0, and thus the predominant absorption mechanism is SA. However, when $I_{00} = 27.0\text{ GW/cm}^2$, $I\beta_{\text{eff}}$ dominates in Eq. (3) and it yields the strong RSA behavior in the CdSe/CdS core/shell NPLs. As a result, the overall nonlinear absorption behavior gradually switches from SA to RSA with increasing the excitation peak intensity. It is believed that such an interesting switching behavior from SA to RSA may provide potential applications in optical pulse compressors and optical switching devices. The SA and RSA behaviors can be used in an optical compressor to reduce the leading edge and trailing edge of a pulse respectively and thus shorten the pulse.^[37] Moreover, considering two single laser beams of four different input combinations (0, 0), (0, 1), (1, 0), (1, 1), we can obtain a logic

0 or 1 by defining a suitable threshold and realize an all-optical exclusive-OR logic gate based on the SA to RSA transition.^[38]

In summary, we have provided a comprehensive understanding of the nonlinear absorption behaviors of CdSe-based NPLs using ps pulses at 532 nm. The CdSe NPLs exhibit a strong RSA behavior resulting from two-photon induced FCA in a nonresonant region. The growth of a monolayer of CdS on the CdSe core can effectively make the absorption band red shift to realize the resonant nonlinear absorption and hence incur completely different nonlinear absorption properties. In detail, the CdSe/CdS core/shell NPLs show an optical switching behavior from SA to RSA with increasing the laser intensity, which are ascribed to the ground state bleaching and FCA, respectively. From the study, it can be seen that CdSe-based NPLs are promising nonlinear optical materials for applications in optoelectronic devices.

References

- [1] Pan L Y et al 2007 *Appl. Phys. Lett.* **91** 051902
- [2] Scott R et al 2015 *Nano Lett.* **15** 4985
- [3] Zhao S L et al 2016 *Opt. Laser Technol.* **82** 104
- [4] Guzelurk B et al 2014 *ACS Nano* **8** 6599
- [5] She C X et al 2014 *Nano Lett.* **14** 2772
- [6] Qu S L et al 2002 *Chem. Phys. Lett.* **356** 403
- [7] Suchand Sandeep C S et al 2010 *Chem. Phys. Lett.* **485** 326
- [8] Huang T et al 2008 *Chem. Phys. Lett.* **451** 213
- [9] Salah A et al 2015 *Appl. Surf. Sci.* **353** 112
- [10] Wang F et al 2010 *Analyst* **135** 1839
- [11] Gerdova I and Haché A 2005 *Opt. Commun.* **246** 205
- [12] Achtstein A W et al 2013 *J. Phys. Chem. C* **117** 25756
- [13] King G C et al 2010 *Appl. Phys. Lett.* **97** 061112
- [14] Ithurria S and Dubertret B 2008 *J. Am. Chem. Soc.* **130** 16504
- [15] Feng X B and Ji W 2009 *Opt. Express* **17** 13140
- [16] Zeng Y et al 2013 *Appl. Phys. Lett.* **102** 043308
- [17] Ithurria S and Talapin D V 2012 *J. Am. Chem. Soc.* **134** 18585
- [18] Achtstein A W et al 2015 *J. Phys. Chem. C* **119** 20156
- [19] Yeltik A et al 2015 *J. Phys. Chem. C* **119** 26768
- [20] Sheik-Bahae M et al 1990 *IEEE J. Quantum Electron.* **26** 760
- [21] Chen X B et al 2003 *Nano Lett.* **3** 799
- [22] Cherevko S A et al 2013 *Phys. Rev. B* **88** 041303
- [23] Ma Y Z et al 2012 *Appl. Opt.* **51** 5432
- [24] He J et al 2005 *Opt. Express* **13** 9235
- [25] Rao S V et al 2011 *Chem. Phys. Lett.* **514** 98
- [26] Sutherland R L et al 2005 *J. Opt. Soc. Am. B* **22** 1939
- [27] Gu. B et al 2008 *Appl. Phys. Lett.* **92** 091118
- [28] Sippel P et al 2015 *Nano Lett.* **15** 2409
- [29] Liu Z B et al 2008 *Adv. Mater.* **20** 511
- [30] Eshet H et al 2013 *Nano Lett.* **13** 5880
- [31] Sreeramulu V et al 2014 *J. Phys. Chem. C* **118** 30333
- [32] Chen J L T et al 2014 *New J. Chem.* **38** 985
- [33] Lee Y H et al 2009 *Appl. Phys. Lett.* **95** 023105
- [34] Gao Y C et al 2005 *Opt. Commun.* **251** 429
- [35] Wang J et al 2010 *Opt. Commun.* **283** 3525
- [36] Ma Y J et al 2011 *Opt. Lett.* **36** 3431
- [37] Band Y B et al 1986 *Chem. Phys. Lett.* **126** 280
- [38] Roy S and Yadav C 2013 *Appl. Phys. Lett.* **103** 241113

Chinese Physics Letters

Volume 34

Number 9

September 2017

GENERAL

- 090101 **Discovery of Fractionalized Neutral Spin-1/2 Excitation of Topological Order** [Views & Comments](#)
Xiao-Gang Wen
- 090201 **Soliton Solutions to the Coupled Gerdjikov–Ivanov Equation with Rogue-Wave-Like Phenomena**
Jian-Bing Zhang, Ying-Yin Gongye, Shou-Ting Chen
- 090202 **A Multi-Symplectic Compact Method for the Two-Component Camassa–Holm Equation with Singular Solutions**
Xiang Li, Xu Qian, Bo-Ya Zhang, Song-He Song
- 090301 **Sound Wave of Spin–Orbit Coupled Bose–Einstein Condensates in Optical Lattice**
Xu-Dan Chai, Zi-Fa Yu, Ai-Xia Zhang, Ju-Kui Xue
- 090302 **Space-to-Ground Quantum Key Distribution Using a Small-Sized Payload on Tiangong-2 Space Lab** [Express Letter](#)
Sheng-Kai Liao, Jin Lin, Ji-Gang Ren, Wei-Yue Liu, Jia Qiang, Juan Yin, Yang Li, Qi Shen, Liang Zhang, Xue-Feng Liang, Hai-Lin Yong, Feng-Zhi Li, Ya-Yun Yin, Yuan Cao, Wen-Qi Cai, Wen-Zhuo Zhang, Jian-Jun Jia, Jin-Cai Wu, Xiao-Wen Chen, Shan-Cong Zhang, Xiao-Jun Jiang, Jian-Feng Wang, Yong-Mei Huang, Qiang Wang, Lu Ma, Li Li, Ge-Sheng Pan, Qiang Zhang, Yu-Ao Chen, Chao-Yang Lu, Nai-Le Liu, Xiongfeng Ma, Rong Shu, Cheng-Zhi Peng, Jian-Yu Wang, Jian-Wei Pan
- 090401 **Effects of Homogeneous Plasma on Strong Gravitational Lensing of Kerr Black Holes**
Chang-Qing Liu, Chi-Kun Ding, Ji-Liang Jing
- 090601 **Direct Digital Frequency Control Based on the Phase Step Change Characteristic between Signals**
Zhao-Min Jia, Xu-Hai Yang, Bao-Qi Sun, Xiao-Ping Zhou, Bo Xiang, Xin-Yu Dou
- 090602 **Transportable 1555-nm Ultra-Stable Laser with Sub-0.185-Hz Linewidth**
Zhao-Yang Tai, Lu-Lu Yan, Yan-Yan Zhang, Xiao-Fei Zhang, Wen-Ge Guo, Shou-Gang Zhang, Hai-Feng Jiang
- 090701 **Terahertz Direct Detectors Based on Superconducting Hot Electron Bolometers with Microwave Biasing**
Shou-Lu Jiang, Xian-Feng Li, Run-Feng Su, Xiao-Qing Jia, Xue-Cou Tu, Lin Kang, Biao-Bing Jin, Wei-Wei Xu, Jian Chen, Pei-Heng Wu

NUCLEAR PHYSICS

- 092101 **Collective Flows of $^{16}\text{O}+^{16}\text{O}$ Collisions with α -Clustering Configurations**
Chen-Chen Guo, Wan-Bing He, Yu-Gang Ma

FUNDAMENTAL AREAS OF PHENOMENOLOGY(INCLUDING APPLICATIONS)

- 094101 **Effects of Breaking Waves on Composite Backscattering from Ship-Ocean Scene**
Jin-Xing Li, Min Zhang, Peng-Bo Wei
- 094201 **High-Order-Harmonic Generation from a Relativistic Circularly Polarized Laser Interacting with Over-Dense Plasma Grating**
Xia-Zhi Li, Hong-Bin Zhuo, De-Bin Zou, Shi-Jie Zhang, Hong-Yu Zhou, Na Zhao, Yue Lang, De-Yao Yu
- 094202 **Cadmium Selenide Polymer Microfiber Saturable Absorber for Q-Switched Fiber Laser Applications**
A. H. A. Rosol, H. A. Rahman, E. I. Ismail, N. Irawati, Z. Jusoh, A. A. Latiff, S. W. Harun
- 094203 **Leaky Modes in Ag Nanowire over Substrate Configuration**
Yin-Xing Ding, Lu-Lu Wang, Li Yu

094301 Geoacoustic Inversion Using Time Reversal of Ocean Noise

Ji-Xing Qin, Boris Katsnelson, Oleg Godin, Zheng-Lin Li

PHYSICS OF GASES, PLASMAS, AND ELECTRIC DISCHARGES

095201 Heat Flux on EAST Divertor Plate in H-mode with LHCD/LHCD+NBI

Bo Shi, Zhen-Dong Yang, Bin Zhang, Cheng Yang, Kai-Fu Gan, Mei-Wen Chen, Jin-Hong Yang, Hui Zhang, Jun-Li Qi, Xian-Zu Gong, Xiao-Dong Zhang, Wei-Hua Wang

CONDENSED MATTER: STRUCTURE, MECHANICAL AND THERMAL PROPERTIES

096101 A Bright Single-Photon Source from Nitrogen-Vacancy Centers in Diamond Nanowires

Shen Li, Cui-Hong Li, Bo-Wen Zhao, Yang Dong, Cong-Cong Li, Xiang-Dong Chen, Ya-Song Ge, Fang-Wen Sun

096201 New Insights on the Deflection and Internal Forces of a Bending Nanobeam

De-Min Zhao, Jian-Lin Liu

096801 Fluorescence Enhancement of Metal-Capped Perovskite $\text{CH}_3\text{NH}_3\text{PbI}_3$ Thin Films

Peng Sun, Wei-Wei Yu, Xiao-Hang Pan, Wei Wei, Yan Sun, Ning-Yi Yuan, Jian-Ning Ding, Wen-Chao Zhao, Xin Chen, Ning Dai

CONDENSED MATTER: ELECTRONIC STRUCTURE, ELECTRICAL, MAGNETIC, AND OPTICAL PROPERTIES

097301 Characterization of Interface State Density of Ni/p-GaN Structures by Capacitance/Conductance-Voltage-Frequency Measurements

Zhi-Fu Zhu, He-Qiu Zhang, Hong-Wei Liang, Xin-Cun Peng, Ji-Jun Zou, Bin Tang, Guo-Tong Du

097302 Fast Electrical Detection of Carcinoembryonic Antigen Based on AlGaIn/GaN High Electron Mobility Transistor Aptasensor

Xiang-Mi Zhan, Quan Wang, Kun Wang, Wei Li, Hong-Ling Xiao, Chun Feng, Li-Juan Jiang, Cui-Mei Wang, Xiao-Liang Wang, Zhan-Guo Wang

097303 Fano Resonance Effect in CO-Adsorbed Zigzag Graphene Nanoribbons

Gao Wang, Meng-Qiu Long, Dan Zhang

097304 Improved Operation Characteristics for Nonvolatile Charge-Trapping Memory Capacitors with High- κ Dielectrics and SiGe Epitaxial Substrates

Zhao-Zhao Hou, Gui-Lei Wang, Jin-Juan Xiang, Jia-Xin Yao, Zhen-Hua Wu, Qing-Zhu Zhang, Hua-Xiang Yin

097305 Evidence of Electron-Hole Imbalance in WTe_2 from High-Resolution Angle-Resolved Photoemission Spectroscopy

Chen-Lu Wang, Yan Zhang, Jian-Wei Huang, Guo-Dong Liu, Ai-Ji Liang, Yu-Xiao Zhang, Bing Shen, Jing Liu, Cheng Hu, Ying Ding, De-Fa Liu, Yong Hu, Shao-Long He, Lin Zhao, Li Yu, Jin Hu, Jiang Wei, Zhi-Qiang Mao, You-Guo Shi, Xiao-Wen Jia, Feng-Feng Zhang, Shen-Jin Zhang, Feng Yang, Zhi-Min Wang, Qin-Jun Peng, Zu-Yan Xu, Chuang-Tian Chen, Xing-Jiang Zhou

097701 Origin of Negative Imaginary Part of Effective Permittivity of Passive Materials

Kai-Lun Zhang, Zhi-Ling Hou, Ling-Bao Kong, Hui-Min Fang, Ke-Tao Zhan

097801 Effect of Droop Phenomenon in InGaIn/GaN Blue Laser Diodes on Threshold Current

Xiao-Wang Fan, Jian-Ping Liu, Feng Zhang, Masao Ikeda, De-Yao Li, Shu-Ming Zhang, Li-Qun Zhang, Ai-Qin Tian, Peng-Yan Wen, Guo-Hong Ma, Hui Yang

CROSS-DISCIPLINARY PHYSICS AND RELATED AREAS OF SCIENCE AND TECHNOLOGY

098101 Nonresonant and Resonant Nonlinear Absorption of CdSe-Based Nanoplatelets

Li-Bo Fang, Wei Pan, Si-Hua Zhong, Wen-Zhong Shen

098701 Temperature Impacts on Transient Receptor Potential Channel Mediated Calcium Oscillations in Astrocytes

Yu-Hong Zhang, Hui Liu, Ying-Rong Han, Ya-Fei Chen, Su-Hua Zhang, Yong Zhan